# A Low-Complexity Detection Scheme for Differential Spatial Modulation

Lixia Xiao, Ping Yang, Xia Lei, Yue Xiao, Shiwen Fan, Shaoqian Li, and Wei Xiang

***Abstract*—Differential spatial modulation (DSM), which does not require the channel state information at the receiver, is an attractive alternative to its coherent counterpart. The optimal maximum-likelihood (ML) detector of the DSM system employs the classic block-by-block method for jointly detecting the activated antenna matrix (AM) and the modulation symbols, resulting in high computational complexity. In this letter, a low-complexity near-ML detector, which operates on a symbol-by-symbol basis, is proposed for the DSM scheme. Specifically, in each block, the index of the activated transmit antenna and modulation symbol in each time slot are first obtained, and then, these antenna indices are utilized to simply determine the index of the activated AM. Simulation results show that the proposed algorithm is capable of offering almost the same performance as that of the ML detector with more than 90% reduction in complexity.**

***Index Terms*—Differential spatial modulation (DSM), maximum-likelihood (ML) detection, symbol-based-symbol.**

## I. Introduction

DIFFERENTIAL SPATIAL MODULATION (DSM) [1]–[4] is a novel multiple-input multiple-output (MIMO) wireless transmission technique, which relies on a single radio-frequency (RF) transmit structure without the need of the channel state information (CSI). It is an attractive alternative to the coherent spatial modulation (SM) [5]–[8], which is considered as a promising transmission technique for large-scale MIMO systems in terms of both theoretical researches and practical implementations [9], [10].

In DSM, one out of $Q$ antenna matrices (AMs) is activated to dispense $N_t$ symbols to $N_t$ transmit antennas (TAs) in $N_t$ time instants. Therefore, high-data transmission is attainable in comparison with the differential space–time shift keying (DSTSK) scheme [11], where only a single symbol is transmitted in a space–time block.

Manuscript received February 17, 2015; accepted June 19, 2015. Date of publication June 23, 2015; date of current version September 4, 2015. This work was supported in part by the National Science Foundation of China under Grant 61471090, by the National Basic Research Program of China under Grant 2013CB329001, by the Fundamental Research Funds for the Central Universities under Grant ZYGX2013J112, by the Program for New Century Excellent Talents in University under Grant NCET-11-0058, and by the Open Research Fund of the National Mobile Communications Research Laboratory, Southeast University, under Grant 2013D05. The associate editor coordinating the review of this paper and approving it for publication was Q. Du.

L. Xiao, P. Yang, X. Lei, S. Fan, and S. Li are with the National Key Laboratory of Science and Technology on Communications, University of Electronic Science and Technology of China, Chengdu 611731, China (e-mail: xiaoyue@uestc.edu.cn; yang.ping@uestc.edu.cn).

Y. Xiao is with the National Key Laboratory of Science and Technology on Communications, University of Electronic Science and Technology of China, Chengdu 611731, China, and also with the National Mobile Communications Research Laboratory, Southeast University, Nanjing 210096, China.

W. Xiang is with the School of Mechanical and Electrical Engineering, University of Southern Queensland, Toowoomba, Qld. 4350, Australia.

Digital Object Identifier 10.1109/LCOMM.2015.2448616

For the current DSM detector, it relies on the classic block-by-block-based maximum-likelihood (ML) detection, where the AM indices and the amplitude and phase modulation (APM) symbols are jointly detected in a space–time block. Hence, the complexity of the ML detector grows exponentially with the size of the constellation set and the number of TAs. Note that some low-complexity non-coherent detectors [11]–[13] have been proposed for DSTSK. However, these detectors are not directly applicable to DSM, because multiple APM symbols are transmitted in a single space–time block in the DSM system. This is also the reason that the low-complexity algorithms designed for coherent detection [14]–[16] are not suitable for DSM systems.

Against this background, a novel low-complexity near ML algorithm, which operates on a symbol-by-symbol basis, is proposed for DSM. The complexity of the proposed detector is independent of the size of the APM symbols. Specifically, the antenna index (AI) and the APM symbol in each time slot are estimated firstly for each space–time block. If the obtained $N_t$ AIs form a legitimate AM, the output is taken as the final detection result. Otherwise, we choose $P$ most likely legitimate AMs for further search. The selection principle is able to maximize the number of identical elements between these AI vectors and the original detected AIs. Furthermore, the proposed algorithm is extended to large-scale DSM-MIMO system with the aid of index mapping proposed in [4].

## II. System Model

Consider a DSM system with $N_t$ transmit and $N_r$ receive antennas. For the DSM scheme, one out of $Q$ AMs is activated to disperse $N_t$ symbols to $N_t$ TAs in $N_t$ time slots. In the DSM system, there are total $N_t!$ AMs. In fact, only $Q = 2^{\lfloor \log_2(N_t!) \rfloor}$ AMs are permitted for conveying information bits, where $\lfloor \cdot \rfloor$ is the floor operator. For each $(N_t \times N_t)$-element full-rank AM, there is only one nonzero element in each column. Hence, each AM $\mathbf{A}_q (q \in (1, Q))$ corresponds to one unique AI vector $\mathbf{L}_q = (l_q^1, l_q^2, \ldots, l_q^{N_t})$, where $l_q^j$, $(j \in (1, N_t))$ is the activated index of the $j$-th column of $\mathbf{A}_q$. Therefore, $Q$ AMs correspond to an AI set with Q vectors, i.e., $\mathbb{L} = (\mathbf{L}_1, \ldots, \mathbf{L}_q, \ldots, \mathbf{L}_Q)$.

For each group of $N_t$ time slots, the information bits of length $B$ are divided into two parts: 1) $B_1 = \log_2(Q)$ bits are used to map one of the AMs $\mathbf{A}_q$; and 2) $B_2 = \log_2(L) N_t$ bits are modulated to $N_t$ $L$-PSK symbols that are transmitted by the activated AM $\mathbf{A}_q$. As a result, the $k$-th space–time block signal is expressed as

$$\mathbf{X}_k = \mathbf{A}_q diag[s_1, s_2 \ldots, s_{N_t}], \tag{1}$$

where $diag[\cdot]$ returns a square diagonal matrix with the elements of vector and $s_j, j \in (1, N_t)$ denotes the $L$-PSK symbol. Differential encoding of DSM can be expressed as

$$\mathbf{S}_k = \mathbf{S}_{k-1} \mathbf{X}_k, \tag{2}$$

TABLE I
SIZES OF $Q$ AND $\chi$ WITH DIFFERENT SYSTEM SETUPS

| $(N_t,L)$ | (4,4) | (6,4) | (6,8) | (8,4) | (8,8) | (16,4) | (16,8) |
|---|---|---|---|---|---|---|---|
| Size of $Q$ | $2^4$ | $2^9$ | $2^9$ | $2^{15}$ | $2^{15}$ | $2^{44}$ | $2^{44}$ |
| Size of $\chi$ | $2^{12}$ | $2^{21}$ | $2^{27}$ | $2^{31}$ | $2^{39}$ | $2^{76}$ | $2^{92}$ |

where $\mathbf{S}_0$ is the $(N_t \times N_t)$-element identity matrix.

At the receiver, the received $k$-th space–time block $\mathbf{Y}_k \in \mathbb{C}^{N_r \times N_t}$ is modeled as

$$\mathbf{Y}_k = \mathbf{H}_k \mathbf{S}_k + \mathbf{n}_k, \tag{3}$$

where $\mathbf{H}_k \in \mathbb{C}^{N_r \times N_t}$ and $\mathbf{n}_k \in \mathbb{C}^{N_r \times N_t}$ denote the channel matrix and the noise matrix, whose elements obey the complex Gaussian distributions $\mathcal{CN}(0, 1)$ and $\mathcal{CN}(0, \sigma^2)$, respectively. Assuming that channel coefficients remain approximately unchanged over $N_t$ time slots, i.e., $\mathbf{H}_{k-1} \approx \mathbf{H}_k$, the received signal $\mathbf{Y}_k$ can be represented as

$$\mathbf{Y}_k = \mathbf{Y}_{k-1}\mathbf{X}_k + \mathbf{N}_k, \tag{4}$$

where $\mathbf{N}_k = \mathbf{n}_k - \mathbf{n}_{k-1}\mathbf{X}_k$. Then the classic block-by-block ML detector can be expressed as

$$(\hat{\mathbf{X}}_k)_{ML} = \arg\min_{\mathbf{X}_k \in \chi} \|\mathbf{Y}_k - \mathbf{Y}_{k-1}\mathbf{X}_k\|^2, \tag{5}$$

where $\chi$ is the set of DSM transmit vectors with a size of $QL^{N_t}$, which is shown in Table I. As can be seen, the sizes of $Q$ and $\chi$ increase exponentially with $L$ and $N_t$.

## III. PROPOSED DETECTION ALGORITHM FOR DSM

### A. Proposed Detection Algorithm

In this section, a novel low-complexity symbol-by-symbol detector is proposed for DSM to attain near-optimal performance with reduced complexity. Specifically, the AI of the TA and the symbol in each time slot are estimated in each time-space block. If the obtained AIs forms a legitimate AM, they alongside the symbol vector are taken as the final results. Otherwise, we choose $P$ most likely legitimate AMs for further search.

Firstly, the $N_t$ AIs and the corresponding symbol vector are estimated. According to Eq. (4), the receiver signal $\mathbf{Y}_k^i \in \mathbb{C}^{N_r \times 1}$, $(i \in (1, N_t))$ can be obtained as

$$\mathbf{Y}_k^i = \mathbf{Y}_{k-1}\mathbf{X}_k^i + \mathbf{N}_k^i, \tag{6}$$

where $\mathbf{Y}_k^i$, $\mathbf{X}_k^i$ and $\mathbf{N}_k^i$ denote the $i$-th column of $\mathbf{Y}_k$, $\mathbf{X}_k$ and $\mathbf{N}_k$, respectively. Since there is only one nonzero element in $\mathbf{X}_k^i$, the activated index and the symbol can be estimated by the HL-ML detector as [16]

$$(\hat{l}_i, \hat{s}_i)_{ML} = \arg\min_{l_i \in (1,\ldots,N_t)} \left( \left| y_k^{l_i} - \hat{s}_i \right|^2 - \left| y_k^{l_i} \right|^2 \right) \left\| \mathbf{Y}_{k-1}^{l_i} \right\|^2, \tag{7}$$

where

$$y_k^{l_i} = \frac{\left(\mathbf{Y}_{k-1}^{l_i}\right)^H \mathbf{Y}_k^i}{\left(\mathbf{Y}_{k-1}^{l_i}\right)^H \mathbf{Y}_{k-1}^{l_i}}, \quad \hat{s}_i = \mathbb{Q}\left(y_k^{l_i}\right), \tag{8}$$

where $\mathbb{Q}$ is defined as the digital demodulation function. After $N_t$ AIs are estimated by Eq. (7), we can obtain the AI vector $\hat{\mathbf{L}}_k = (\hat{l}_1, \ldots, \hat{l}_{N_t})$ and the symbol vector $\hat{\mathbf{s}}_k = (\hat{s}_1, \ldots, \hat{s}_{N_t})$. Then the number of the identical elements between $\hat{\mathbf{L}}_k$ and $\mathbb{L} = (\mathbf{L}_1, \ldots, \mathbf{L}_q, \ldots, \mathbf{L}_Q)$ can be given as

$$\mathbf{N} = [N_1, \ldots, N_q, \ldots, N_Q], \tag{9}$$

where $N_q$ is number of overlapped elements between $\hat{\mathbf{L}}_k$ and $\mathbf{L}_q$. Then the element in $\mathbf{N}$ is sorted in descending order as $\hat{\mathbf{N}} = [\hat{N}_1, \ldots, \hat{N}_q, \ldots, \hat{N}_Q]$, and the corresponding index order is given by

$$\mathbf{m} = [m_1, \ldots, m_q, \ldots, m_Q], \tag{10}$$

where $m_1$ and $m_Q$ denote the indices of $\hat{N}_1$ and $\hat{N}_Q$, respectively. If the condition of $\hat{N}_1 = N_t$ is satisfied, the obtained $\hat{\mathbf{L}}_k$ is considered as a legitimate solution, and thus the achieved $(m_1, \hat{\mathbf{s}}_k)$ is taken as the final output.

If $\hat{N}_1 < N_t$, $\hat{\mathbf{L}}_k$ is considered as a illegitimate solution. Moreover, the largest element in $\mathbf{N}$ may not be unique, and we define $Q_M$ as the number of the largest elements in $\mathbf{N}$. In this case, we choose first $P(P \geqslant Q_M)$ legitimate AMs in Eq. (10) for detection, which can be expressed as

$$(\hat{q}) = \arg\min_{q \in (m_1,\ldots,m_P)} \left\| \mathbf{Y}_k - \mathbf{Y}_{k-1}\mathbf{A}_q diag(\hat{\mathbf{s}}_q) \right\|^2, \tag{11}$$

where $\hat{\mathbf{s}}_q = (s_q^1, s_q^2, \ldots, s_q^{N_t})$ is obtained using Eq. (8).

### B. Extended Version for Large-Scale DSM-MIMO

As shown in Table I, the size of $Q$ grows exponentially as the number of TAs increases. This makes the design of the AMs to become a challenge. To tackle this issue, an effective method of index mapping principle for DSM was introduced in [4]. In this subsection, we extend the proposed algorithm in Section III-A to large-scale DSM systems by using the mapping method. The extension to large-scale DSM focuses mainly on searching $Q_M$ legitimate AMs, which are most likely to be the obtained $\hat{\mathbf{L}}_k$.

*1) Index Mapping of Large-Scale DSM-MIMO:* As shown in [4], given a length of $B_1 = \log_2(Q)$ bits denoted by a binary sequence $[a_1^{(m)}, \ldots, a_{B_1}^{(m)}]$, they are firstly transformed into a decimal integer $m \in (0, Q-1)$. Then, the number $m$ is expressed in factorial representation as

$$m = b_1^{(m)}(N_t - 1)! + \cdots + b_{N_t}^{(m)} 0!, \tag{12}$$

where $\mathbf{b}^{(m)} = (b_1^{(m)}, \ldots, b_{N_t}^{(m)})$ denotes the corresponding factorial sequence. In [4], the sequence $\mathbf{b}^{(m)}$ is mapped to a permutation vector $\mathbf{L}_q = (l_q^1, l_q^2, \ldots, l_q^{N_t})$. Specifically, we first have $l_q^1 = \theta_{b_1^{(m)}}$, where $\theta = [1, 2, \ldots, N_t]$. Then, the element $\theta_{b_1^{(m)}}$ is removed from the set $\theta$, so that we have $l_q^2 = \theta_{b_2^{(m)}}$. After that, $\theta_{b_2^{(m)}}$ is removed from $\theta$. This process is repeated until $l_q^{N_t}$ is obtained.

*2) Index De-Mapping of Large-Scale DSM-MIMO:* For a legitimate AI vector $\mathbf{L}_q$, it is de-mapped to a factorial sequence $\mathbf{b}^{(m)} = (b_1^{(m)}, \ldots, b_{N_t}^{(m)})$ in [4]. Specifically, $\hat{l}_{N_t}$ is firstly added

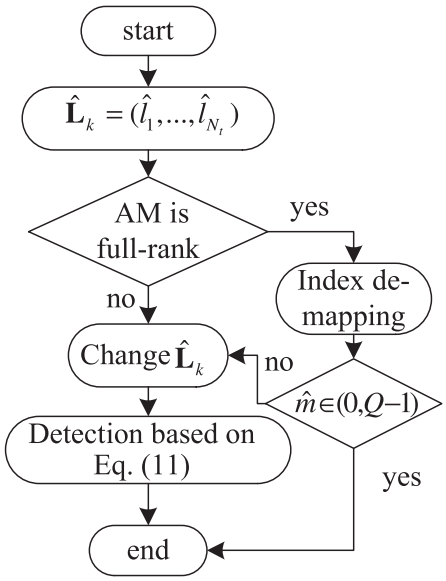


Fig. 1. The process of the extended detector for large-scale DSM.

to $\tilde{\theta}$, which is initialized as an empty vector and we have $b_{N_t}^{(m)} = 0$. Then the term $\hat{l}_{N_t-1}$ is added to the set $\tilde{\theta}$, which is then sorted in ascending order. After that, the index of $\hat{l}_{N_t-1}$ in the ordered $\tilde{\theta}$ is obtained as $\ell_{N_t-1}$ and we have $b_{N_t-1}^{(k)} = \ell_{N_t-1} - 1$. This process is repeated until $b_1^{(m)}$ is obtained. Finally, the obtained vector $\mathbf{b}^{(m)}$ can be transformed to an integer $\hat{m}$.

*3) Extension of the Proposed Algorithm:* The proposed algorithm in Section III-A is extended to large-scale DSM-MIMO systems with the aid of index mapping and de-mapping, as shown in Fig. 1. As can be seen from the figure, one first checks whether the estimated $\hat{\mathbf{L}}_k$ is legitimate through index mapping and de-mapping. When $\hat{\mathbf{L}}_k$ falls within the legitimated set, it is mapped to a corresponding AM. If the resultant AM is a full-rank matrix, and the de-mapped $\hat{m}$ satisfies that $\hat{m} \in (0, Q-1)$, $(\hat{m}, \hat{\mathbf{s}}_k)$ is taken as the final solution. Otherwise, the obtained $\hat{\mathbf{L}}_k$ is regarded as illegitimate, and one modifies some elements in $\hat{\mathbf{L}}_k$ following the principle of maximizing the number of identical elements between the modified AI vector and the obtained $\hat{\mathbf{L}}_k$. Finally, all the legitimate AMs are selected for detection using Eq. (11).

In Fig. 1, if the AM is full rank and the de-mapped number satisfies $\hat{m} > (Q-1)$, the most likely erroneous AI is found according to the index de-mapping factorial sequence $\mathbf{b}^{(m)}$, and then amended to other legitimate values. According to Eq. (12), the inequality of $b_j^{(m)}(N_t - j)! \leqslant m - (b_1^{(m)}(N_t-1)!+, \ldots, +b_{j-1}^{(m)}(N_t - j + 1)!)$ should hold for the estimated $b_j^{(m)}$. Otherwise, the index $\hat{l}_j$ in vector $\hat{\mathbf{L}}_k$ may be incorrect. In this case, we exchange $\hat{l}_j$ with $\hat{l}_{j+1}, \ldots, \hat{l}_{N_t}$, respectively, to obtain $N_t - j$ changed AI vectors, corresponding to $N_t - j$ possible AMs.

On the other hand, if the AM is not a full-rank matrix, this implies that some elements in $\hat{\mathbf{L}}_k$ are identical, and hence some AIs are not included in the set $\hat{\mathbf{L}}_k$. In this case, we replace these identical elements in $\hat{\mathbf{L}}_k$ with these non-included AIs to make the AM to be a full-rank matrix. Assume that there are $t$ groups of repeated AIs and $\hat{n}_t$ non-included AIs. These $\hat{n}_t$ non-included AIs are able to form $\hat{n}_t!$ combinations.

For these elements of $t$ groups, we keep only one element for each, the rest elements are substituted by the remaining $\hat{n}_t$ indices. Assuming that each group has $n_i (i \in (1, t))$ identical elements, there are $\prod_{i=1}^{t} n_i \hat{n}_t!$ possible AMs, and all the legitimate AMs are selected for detection. For example, letting the number of the TA be $N_t = 16$ and $\hat{\mathbf{L}}_k = (2, 1, 4, 3, 6, 5, 1, 8, 13, 16, 9, 12, 4, 14, 7, 10)$, we have

$$t = 2 \rightarrow \{1, 1\}, \{4, 4\}, n_1 = 2, n_2 = 2. \tag{13}$$

Then, according to $\hat{\mathbf{L}}_k$, the non-included $\hat{n}_t$ AIs are

$$\hat{n}_t = 2 \rightarrow \{11, 15\}. \tag{14}$$

Hence, there are 8 possible AMs given as

$$\begin{aligned}
\hat{\mathbf{L}}_k^1 &= (2, 1, 4, 3, 6, 5, \mathbf{11}, 8, 13, 16, 9, 12, \mathbf{15}, 14, 7, 10)\\
\hat{\mathbf{L}}_k^2 &= (2, 1, 4, 3, 6, 5, \mathbf{15}, 8, 13, 16, 9, 12, \mathbf{11}, 14, 7, 10)\\
\hat{\mathbf{L}}_k^3 &= (2, 1, \mathbf{11}, 3, 6, 5, \mathbf{15}, 8, 13, 16, 9, 12, 4, 14, 7, 10)\\
\hat{\mathbf{L}}_k^4 &= (2, 1, \mathbf{15}, 3, 6, 5, \mathbf{11}, 8, 13, 16, 9, 12, 4, 14, 7, 10)\\
\hat{\mathbf{L}}_k^5 &= (2, \mathbf{15}, 4, 3, 6, 5, 1, 8, 13, 16, 9, 12, \mathbf{11}, 14, 7, 10)\\
\hat{\mathbf{L}}_k^6 &= (2, \mathbf{11}, 4, 3, 6, 5, 1, 8, 13, 16, 9, 12, \mathbf{15}, 14, 7, 10)\\
\hat{\mathbf{L}}_k^7 &= (2, \mathbf{11}, \mathbf{15}, 3, 6, 5, 1, 8, 13, 16, 9, 12, 4, 14, 7, 10)\\
\hat{\mathbf{L}}_k^8 &= (2, \mathbf{15}, \mathbf{11}, 3, 6, 5, 1, 8, 13, 16, 9, 12, 4, 14, 7, 10)
\end{aligned} \tag{15}$$

In summary, denote by $\hat{Q}_M$ the number of legitimate AMs corresponding to the changed AI vectors in the large-scale DSM-MIMO detection. $\hat{Q}_M$ may be larger than $Q_M$ obtained by Eq. (10), which imposes extra complexity. However, this extension will still be attractive for large-scale DSM-MIMO detection, as shown in Section IV.

### C. Complexity Analysis

The complexities of the proposed algorithm and the ML detector are evaluated in terms of the number of real-valued multiplications, which can be counted as

$$\begin{aligned}
C_{proposed} &= C_1\gamma_1 + \gamma_2\left(C_1 + \left(2N_rN_t + 4N_rN_t^2\right)P\right)\\
C_{ML} &= (4N_rN_t + 2N_rN_t)2^{\lfloor \log_2(N_t!) \rfloor} L^{N_t},
\end{aligned} \tag{16}$$

where $C_1 = (6N_r + 11)N_t + (4N_r + 11)N_t(N_t - 1)$ is the complexity of the proposed detector with legitimate $\hat{\mathbf{L}}_k$, $\gamma_1$ and $\gamma_2$ $(\gamma_1 + \gamma_2) = 1$ denote the percentages of legitimate and illegitimate $\hat{\mathbf{L}}_k$, respectively. As shown in Eq. (16), the complexity of the proposed detector is independent of the size of APM symbols, and dominated by $\gamma_1$, $\gamma_2$ and $P$.

## IV. Simulation Results

In this section, computer simulation are carried out over Rayleigh flat fading channels. Fig. 2 plots the bit error rate

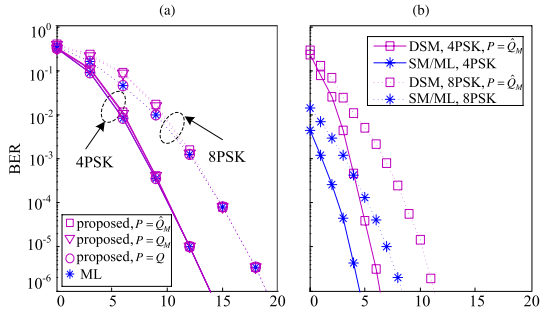


Fig. 2. BER performance of DSM with different antennas configurations: (a) $N_t = 6, N_r = 6$. (b) $N_t = 16, N_r = 16$.

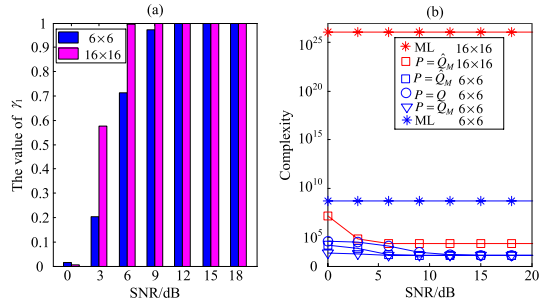


Fig. 3. Percentage of legitimate $\hat{\mathbf{L}}_k$ and the complexity of the proposed detector aided 4-PSK at $N_t = 6, N_r = 6$ and $N_t = 16, N_r = 16$. (a) Percentage. (b) Complexity.

(BER) of the DSM system with $N_t = 6$ and $N_t = 16$ using the proposed detector. For comparative purposes, the curves of ML detector of DSM and SM with perfect CSI are added to Fig. 2(a) and (b), respectively. Furthermore, the BER performance and the complexity of the proposed algorithm are dominated by $\gamma_1$, as shown in Fig. 3(a). These values of $\gamma_1$ are statistic simulation results and equivalent to $r_1/r$, where $r_1$ is the number of legitimate $\hat{\mathbf{L}}_k$ and $r$ is the total number of legitimate and illegitimate $\hat{\mathbf{L}}_k$. Finally, the complexity comparison between the proposed detector and the ML detector is shown in Fig. 3(b).

As can be seen from Fig. 3(a), $\gamma_1$ increases with the SNR. Specifically, $\gamma_1$ is able to reach 100% at the SNRs of 12 dB and 6 dB with $N_t = 6$ and $N_t = 16$, respectively. When the condition $\gamma_1 = 100\%$ is met, the performance of the proposed detector is the same as that of the ML detector. Meanwhile, $\gamma_2$ decreases as SNR increases, and approaches zero at high SNRs. As a result, the complexity of the proposed detector drops as the SNR increases, and becomes a constant at high SNRs, which is shown in Fig. 3(b). Furthermore, although the complexity of the proposed detector increases as the parameter $P$ increases at low SNRs, the proposed detector with $P = Q$ is still able to achieve more than 90% complexity reduction over the ML detector.

At low SNRs, the value of $\gamma_1$ is not equal to 100%, implying that there are inaccurate AIs in $\hat{\mathbf{L}}_k$. Since the proposed detectors with $P = Q_M$ and $P = \hat{Q}_M$ are both designed based on the same location maximization criterion, the accurate AM may be contained in the selected $Q_M$ or $\hat{Q}_M$ AMs. This is the main reason that the proposed detectors with $P = Q_M$ and $P = \hat{Q}_M$ have negligible performance losses compared with the ML detector at low SNRs, which can be seen from Fig. 2(a). As expected, the proposed detector with $P = Q$ always performs as well as the ML detector.

As for large-scale DSM detection with $N_t = 16$, where the ML detector for DSM is computational intractable, the proposed algorithm with $P = \hat{Q}_M$ still performs well, and has only about 2 dB performance loss compared to coherent ML detection.

## V. Conclusion

This letter proposed a low-complexity detector based on symbol-by-symbol detection for the DSM system. Compared to the classic block-by-block based ML detector, the proposed detector is capable of achieving near the same BER performance with significantly reduced complexity. In future, the impact of potential bandwidth expansion [17] of DSM system will be investigated, so as to improve the performance of the detector under band-limited scenarios.

## References

[1] Y. Bian, M. Wen, X. Cheng, H. V. Poor, and B. Jiao, "A differential scheme for spatial modulation," in *Proc. IEEE Globecom. Conf.*, Atlanta, GA, USA, Dec. 2013, pp. 3925–3930.
[2] M. Wen *et al.*, "Performance analysis of differential spatial modulation with two transmit antennas," *IEEE Commun. Lett.*, vol. 18, no. 3, pp. 475–478, Mar. 2014.
[3] N. Ishikawa and S. Sugiura, "Unified differential spatial modulation," *IEEE Wireless Commun. Lett.*, vol. 3, no. 4, pp. 337–340, Feb. 2014.
[4] Y. Bian *et al.*, "Differential spatial modulation," *IEEE Trans. Veh. Technol.*, vol. 64, no. 7, pp. 3262–3268, Jul. 2015.
[5] R. Mesleh, H. Haas, S. Sinanovic, C. W. Ahn, and S. Yun, "Spatial modulation," *IEEE Trans. Veh. Technol.*, vol. 57, no. 4, pp. 2228–2241, Jul. 2008.
[6] M. Di Renzo, H. Haas, and P. M. Grant, "Spatial modulation for multiple-antenna wireless systems: A survey," *IEEE Commun. Mag.*, vol. 49, no. 12, pp. 182–191, Dec. 2011.
[7] M. Di Renzo, H. Haas, A. Ghrayeb, S. Sugiura, and L. Hanzo, "Spatial modulation for generalized MIMO: Challenges, opportunities and implementation," *Proc. IEEE*, vol. 102, no. 1, pp. 56–103, Jan. 2014.
[8] P. Yang, M. Di Renzo, Y. Xiao, S. Q. Li, and L. Hanzo, "Design guidelines for spatial modulation," *IEEE Commun. Tuts. Surveys*, vol. 17, no. 1, pp. 1–24, May 2014.
[9] N. Serafimovski *et al.*, "Practical implementation of spatial modulation," *IEEE Trans. Veh. Technol.*, vol. 62, no. 9, pp. 4511–4523, Nov. 2013.
[10] A. Younis *et al.*, "Performance of spatial modulation using measured real-world channels," in *Proc. IEEE Veh. Technol. Conf.*, Las Vegas, NV, USA, Sep. 2013, pp. 1–5.
[11] S. Sugiura, S. Chen, and L. Hanzo, "Coherent and differential space–time shift keying: A dispersion matrix approach," *IEEE Trans. Commun.*, vol. 58, no. 11, pp. 3219–3230, Nov. 2010.
[12] C. Xu, S. Sugiura, S. X. Ng, and L. Hanzo, "Reduced-complexity non-coherent detected differential space–time shift keying," *IEEE Signal Process. Lett.*, vol. 18, no. 3, pp. 153–156, Mar. 2011.
[13] S. Sugiura, C. Xu, S. X. Ng, and L. Hanzo, "Reduced-complexity coherent versus noncoherent QAM-aided space–time shift keying," *IEEE Trans. Commun.*, vol. 59, no. 11, pp. 3090–3101, Nov. 2011.
[14] A. Younis, S. Sinanovic, M. Di Renzo, R. Y. Mesleh, and H. Haas, "Generalised sphere decoding for spatial modulation," *IEEE Trans. Commun.*, vol. 61, no. 7, pp. 2805–2815, Jul. 2013.
[15] Q. Tang, Y. Xiao, P. Yang, Q. Yu, and S. Li, "A new low-complexity near-ML Detection algorithm for spatial modulation," *IEEE Wireless Commun. Lett.*, vol. 2, no. 1, pp. 90–93, Feb. 2013.
[16] R. Rajashekar, K. V. S. Hairi, and L. Hanzo, "Reduced-complexity ML detection and capacity-optimized training for spatial modulation systems," *IEEE Trans. Commun.*, vol. 62, no. 1, pp. 112–125, Jan. 2014.
[17] K. Ishibashi and S. Sugiura, "Effects of antenna switching on band-limited spatial modulation," *IEEE Wireless Commun. Lett.*, vol. 3, no. 4, pp. 345–348, Apr. 2014.